Workshop on Visualisation in Environmental Sciences (EnvirVis) (2019)
R. Bujack and K. Feige and K. Rink and D. Zeckzer (Editors)

Topology-based Feature Detection in Climate Data

C. P. Kappe[1] M. Böttinger[2] and H. Leitte[1]

[1]TU Kaiserslautern, Department of Computer Science, Germany
[2]Deutsches Klimarechenzentrum (DKRZ), Germany

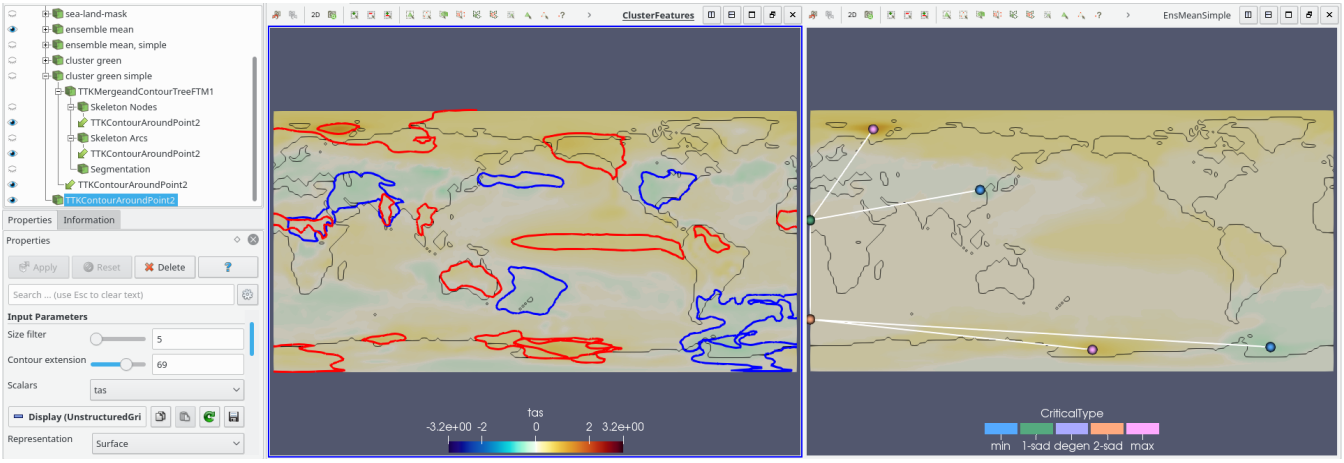

Figure 1: *ParaView session with the MPI-GE temperature anomaly dataset, time 1969-07-01. We have loaded the ensemble mean and the means of two previously computed clusters (subgroups of the ensemble). Left: pipeline and parameter view with our new filter. middle: ensemble mean overlayed with the features of two clusters. right: simplified ensemble mean overlayed with the corresponding contour tree. We see cluster agreement in the north west and south east, opposing trends in Africa and India, and several cluster-specific features.*

Abstract

The weather and climate research community needs to analyze increasingly large datasets, mostly obtained by observations or produced by simulations. Ensemble simulation techniques, which are used to capture uncertainty, add a further dimension to the multivariate time-dependent 3D data, even tightening the challenge of finding relevant information in the data for answering the respective research questions. In this paper we propose a topology-based method to support the visual analysis of climate data by detecting regions with particularly strong local minima or maxima and highlighting them with colored contours. Combined with preceding clustering of the data fields, typical spatial patterns characterizing the climate variability are detected and visualized. We demonstrate the utility of our method with a study of global temperature anomalies of a 150-years ensemble simulation consisting of 100 members.

CCS Concepts

• ***Human-centered computing*** → ***Geographic visualization;*** • ***Applied computing*** → ***Environmental sciences;***

1. Introduction

To capture uncertainty and thereby enhance the practical value of weather and climate simulations, ensemble techniques are regularly applied in both domains today (see e.g. [BTB15] and [BSTS16]). The larger ensembles are, the statistically more robust are the results. At the same time, the probability of capturing rare events rises. As an example, for capturing a 1000-year flood, i.e., a flood that occurs statistically once in 1000 years, 1000 model years need statistically to be computed. However, large climate or weather ensembles are quite challenging with regard to their computational costs, the storage space needed, and the analysis of the resulting

DOI: 10.2312/envirvis.20191099

large and complex data. The visual analysis of ensemble simulations is generally challenging since the data includes the uncertainty dimension additionally to the spatial dimensions and the temporal one [BPR*15].

This additional dimension is often used to derive a robust ensemble mean field that is presented as the ensemble simulation's result. To take the probability distribution of the ensemble into account, the median or percentiles are also often used to provide a result range together with the respective probabilities. Further uses are derived climate indices that can be used to study and communicate the development of climate extremes.

In this work, we focus on the detection of global climate patterns defined by the position and size of specific regions that show stronger or weaker signals compared to the global mean. The approach we take aims to capture the "fingerprints" of distinct climate patterns one often tries to make out in a dataset and whose presence has previously only been judged subjectively.

The method proposed in this paper is applicable to single scalar fields, multi-fields and whole scalar field ensembles. In the latter case, the visualization becomes a kind of spaghetti plot that potentially suffers from visual clutter. Therefore, in the study in Section 5, we build upon a preceding clustering, that summarizes ensemble members, leaving us with only a handful of fields to compare with each other and against the complete ensemble mean.

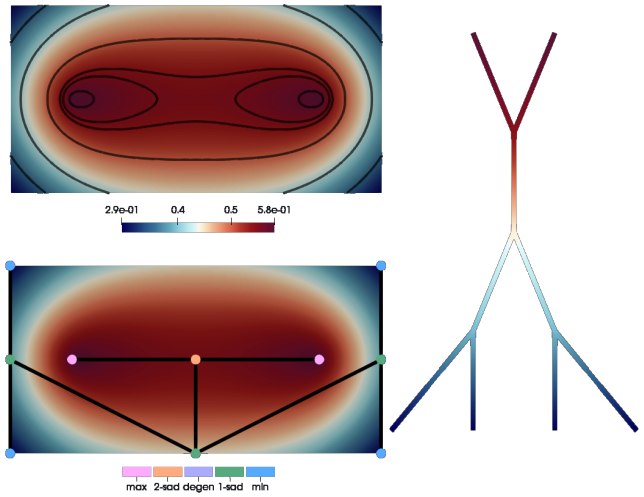

Figure 2: *Basic concepts used in our approach. Top left: black contours for decreasing isovalues from inner to outer parts of the domain. Bottom left: the contour tree embedded in the domain (edges connecting critical points). Right: the same contour tree visualized with y-coordinate and color reflecting the scalar values.*

2. Background

For this work we used the new "Grand Ensemble" (MPI-GE) of the Max-Planck-Institute for Meteorology, which is up to date one of the largest ensemble climate simulations carried out with a comprehensive Earth system model (MPI-ESM1.1) using a horizontal grid resolution of approximately 180 km [Ste15, BSTS16]. In addition to a 2000 year control experiment, the historical past (1850-2005) and three future scenarios for the time 2005-2100 (RCP8.5, RCP4.5 and RCP2.6 plus one experiment with 1 percent CO_2 increase per year) were simulated with an ensemble size of 100. We chose to work with the anomaly of the monthly mean temperature at 2 meters height of the historical experiment. In particular, in this paper, we only deal with 2D domains (like the surface of the earth) but the method theoretically also works for volumetric data.

The method we propose in this paper is based on scalar field topology. In the following paragraphs, we give brief explanations of the concepts needed to understand our approach; generally, topological analysis has been used in a lot of visualization research, over which the survey by Heine et al. gives an overview [HLH*16] also explaining the methodology quite thoroughly.

An important notion in topology are *isocontours*. These are subsets of the domain where the scalar function takes on the same value (the so-called isovalue). In 2D, isocontours are lines that do not self-intersect and are either closed loops or end on the domain boundary. A typical example where isolines are used for visualization is contour maps that depict the elevation in geographical maps. See Figure 2 top left for a simple example. Any isocontour encloses a region. So, given a specific isovalue, one can find a disjoint set of such regions. It is often useful to know how many different regions exist in a dataset for a certain isovalue and how they are nested within regions corresponding to another isovalue. In our example, there are two mountain tips for a high value that are both part of one larger region for a lower value; going even lower (the white-blue range), the domain is split into a left and right part and eventually the four corners are separated. This merging and splitting is modeled in the *contour tree* [GFJT17] that can be computed for any scalar field. Naturally, its leaves are the extrema in the scalar field, which is where the regions shrink to a single point as in Figure 2.

3. Related Work

With the increase in available computing power in the past decade that enabled carrying out ensemble simulations on a routinely basis, the field of ensemble and uncertainty visualization has received more and more attention. Section 5.7 in [RBS*18] gives an in-depth overview on the state of ensemble visualization in meteorology.

There are several papers concerned with the detection of features in field data and/or the comparison of fields based on them. The topic is related to the problem of segmentation, i.e. dividing a dataset into disjoint regions, and therefore to classification of cells (pixels) in field (image) data. In environmental sciences, such techniques [LW07] are used to create a thematic map from remotely sensed data, e.g. different classes of land-use [GMH92].

In meteorology, pattern recognition techniques are used to detect and track storms, e.g. [Wil81, Hod94, BRTM16]. Here, sometimes features are just single points, as opposed to regions of some extent, which we are interested in. In "Extracting Spatio-Temporal Patterns from Geoscience Datasets" [MMS*94], the signature of an extra-tropical cyclone is defined as a set of closed contours surrounding a minimum in sea level pressure.

Generally, we follow the approach of Silver [Sil95] in this paper, who has identified extrema in scalar fields as good seed points for regions that can be regarded features. Over the years this research direction has successfully been further pursued. With topological analysis, the concept has been rooted in a solid mathematical framework. In particular, the notion of *largest contours* [MHS*96] has specified good boundaries for regions grown from extreme points. (We give more details about this approach in Section 4.1.) In the *flexible isosurfaces* system [CSvdP10] isovalues that are well-suited for a visualization are selected based on a contour tree that has been simplified w.r.t. a certain *local geometric measure* like volume or height. Features defined as largest contours computed from a simplified contour tree have also been used to study fluid flow. To this end, meaningful scalar variables (like vorticity) are derived from the vector field and two [SWC*08] or more [SHCS13] of them are compared. This includes a quantitative similarity measure as well as a rendering of the (typically overlapping) respective contours. In a recent paper [FFST19], Tierny et al. propose a novel visualization for scalar field ensembles also based on comparing critical points. Ensemble climate simulations have also been analyzed with *Pareto sets* [HFBG17], a concept similar to largest contours for multivariate data.

Pattern recognition methods have been used in climate sciences for different purposes. The works of [Has93, HvSH*96] gained some publicity due to their political implications; they showed for the first time with statistical methods that the observed temperature increase could for a large part be attributed to human activities causing greenhouse gas emissions. Here, *optimal fingerprints*, i.e. scalar fields with maximal signal-to-noise ratio derived from time-dependent climate simulations, could explain the temperature changes observed to that date. According fingerprints of simulations only taking natural variability into account, however, couldn't explain the observed temperature change patterns.

The method is related to *Empirical Orthogonal Functions* [HJS07], which represent a dataset as a series of scalar fields of which the first ones capture the most distinguished features of the dataset while the others are typically disregarded eventually in order to reduce the dimensionality of the original signal. Using clustering (k-means or other algorithms), the individual fields of climate ensembles have been divided into groups representing different climate states or trends [OBJ16, KBL18].

4. Method

In this section we describe our method of computing and visualizing regions of interest, which we also call features, in scalar fields.

4.1. Computation

The basic idea of our method is that typical patterns found in climate data are often characterized by the occurrence of extraordinary low or high values in scalar variables such as temperature, precipitation or pressure in specific regions. This makes local minima and maxima good candidates for starting points regarding the search for regions of interest, because they are by definition lower/higher than their immediate neighborhood. However, depending on the variable chosen, small scale variations cause "false positives" to be found, i.e. a large number of local extrema as shown in Figure 3. To focus on only the relevant points, the high-frequent noise has to be removed. This is achieved by *topological simplification* [ELZ00, TP12]. This technique basically simplifies the contour tree by removing some of its vertices, and then adapts the scalar field accordingly.

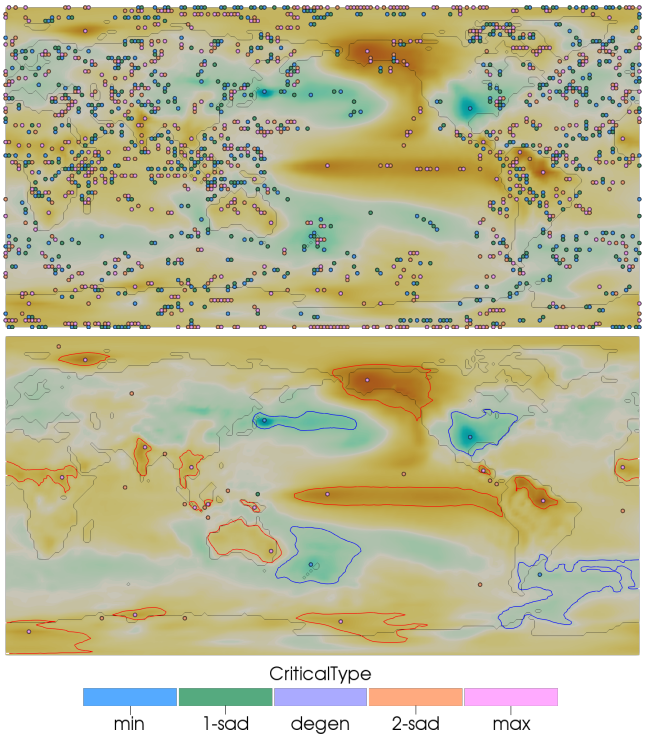

Figure 3: *Time 1969-07-01 in the MPI-GE dataset, orange cluster with critical points. Top: raw data; bottom: simplified data, with feature contours.*

There are several criteria imaginable for simplifying the contour tree. We have chosen the *persistence* associated with an edge. This is a measure for the difference (in the scalar variable) between an extreme point and its "surroundings", here clearly defined by the other vertex of the edge. For example, in Figure 2 right, the persistence of a branch is proportional to the vertical space it takes up. We have chosen persistence over other properties (like size) because this is actually a good formalization of the idea of "extraordinary low or high values". So, at this step, we introduce a parameter to control the desired persistence threshold. It is bound between zero and the range of the scalar field; its choice eventually depends on the dataset and application.

The extreme points that remain after the simplification now represent regions significantly different from the field around them. But because the climate phenomena we are interested in are characterized by spatial patterns, we need to further process the located points. Generally, we find it makes sense that the boundary of a feature region is defined by an isocontour (as opposed to e.g. a circle with a fixed radius) so that the feature outline respects the underlying field data, This raises the question how to determine a suitable

isovalue for each feature. At one end of the spectrum of sensible values is the value at the extreme point itself; this would yield a theoretically infinitesimal small region. Concerning the other end of the spectrum, there is the notion of largest contours [MHS*96]: For an unambiguous assignment of domain space to feature region and for an eventually easily readable visualization, it is desirable to have the contours not intersect each other. If f is the scalar function, and (p,q) and (q,r) are edges in the contour tree, p and r being extrema and q being a saddle point, then $f(q) =: \xi$ is the value that defines the largest such isocontour (the contours of p and r touch at q). This is by far the most common case we have encountered in practice; should a minimum and maximum be directly connected (as in Figure 5 bottom right), we define $\xi := (f(p) + f(r))/2$. Because we do not look for a comprehensive segmentation of the domain, and too large regions do not fit the idea one has of these climate features, we introduce a second parameter here, the feature extent $\lambda \in [0,1]$; it defines the isovalue α for a feature seeded at p: $\alpha = f(p) \cdot (1-\lambda) + \xi \cdot \lambda$.

Finally, while we regard it a necessary condition for a feature to be based on a local extremum, one may additionally require a sufficient size. Therefore we have introduced a third parameter that filters out those regions which do not have a minimum size, given relative to the size of the domain.

4.2. Visualization

Being bounded by isocontours, our features are ready to be visualized as isolines in 2D or isosurfaces in 3D. They can be colored uniformly, w.r.t. the isovalue or depending on the category of the extreme point. For our figures we chose the latter approach with blue for minima and red for maxima.

It is possible, especially in 2D, to render isocontours from multiple fields in one image, resulting in so-called spaghetti plots. We have applied this technique with the mean fields computed from ensemble member clusters (see Section 5). Here the opacity of the isolines can be used as a channel to communicate the size of the respective cluster, such that small clusters are (almost) not reflected in the visualization while features from clusters with many members are (fully) opaque. In these spaghetti plots we see (i) similarities between clusters (common features: multiple contours of the same color in proximity), (ii) peculiarities of one cluster (unique features: single contours) and (iii) strong contrasts (opposite features: multiple different-colored contours in proximity). Such a spaghetti plot can be drawn on top of a colormap visualization of the ensemble mean. Even though not explicitly computed, the ensemble mean's own features will also be highlighted if they occur in at least one cluster (as in Figure 6, top row); they appear possibly even more prominent in case (i).

4.3. Implementation

We have implemented the feature computation using the Topology ToolKit (TTK) [TFL*18] as a plugin (filter) for the well-known visualization application ParaView. The visualization of the features can also be done directly in ParaView, as well as many optional, augmenting visualizations (scalar field color mapping for the original and simplified data, extreme points, contour tree). At the time you are reading this, the filter may already be included in the official TTK release.

The main runtime is spent for the computation and simplification of the contour tree; the time spent for the processing of the typically relatively few feature seed points is negligible in comparison. For our 2D data, results were visible virtually instantaneously (later time-steps being handled only on demand). The three parameters mentioned above can be changed interactively.

5. Results

In this section we present results that we obtained when applying our method to the the data introduced in Section 2. In a preprocessing step, we computed a clustering as proposed by Kappe et al. [KBL18]. In this approach, each time step of each ensemble member is assigned a cluster, to reduce the complexity of large ensembles and get a quick overview over its temporal development. The implementation uses k-means clustering [Llo82] where we experimented with several small values for k and eventually found $k = 5$ to yield a good clustering in the sense that the clusters are well-distinguishable from each other while their respective members are all quite similar. In addition to the exported cluster means, we have saved an image of the so-called Clustering Timeline, shown in Figure 4. It indicates that the dataset can roughly be divided into three phases. In the first phase most ensemble members belong either to the blue or the pink cluster; in the second phase these clusters are superseded by the orange and green (yellowish) cluster; in the third phase the whole ensemble is eventually assigned the gray cluster.

For all the field visualizations for this section we have used the same colormap ranging from -3.25 K to 3.25 K in the temperature anomaly, which is mapped to a blue-turquoise-white-yellow-red color scheme. For the feature detection in the presented cases, we set the persistence threshold to 0.35 K. In the following two sections we use our feature visualization to analyze the overall ensemble (Section 5.1) and individual time steps (Section 5.2).

5.1. Time-independent

The means of the five time-independent clusters are shown in Figure 5. The three rows in the figure reflect the three phases revealed by the Clustering Timeline. Just a glance at the colormap visualizations tells us that there is a general trend towards a warmer-than-normal climate.

In general, our feature detection does a good job at detecting the outstanding regions in the scalar fields (as we judge by "manually" inspecting the colormap visualizations). The results in the top row in Figure 5 indicate, however, that the persistence parameter must be chosen carefully. Eventually it is up to the user, how large the difference between an extremum and its surroundings must be to count as a feature. In our example, we have a relatively small scalar range mapped to a relatively wide range of hues which results in regions being quite clearly distinguishable from their surroundings even though there is not much quantitative difference. In such a case our feature detection can serve as a more reliable guidance than the first impression of a simple colormap visualization. Compare, e.g., the Pacific Ocean in the top and middle left in Figure 5.

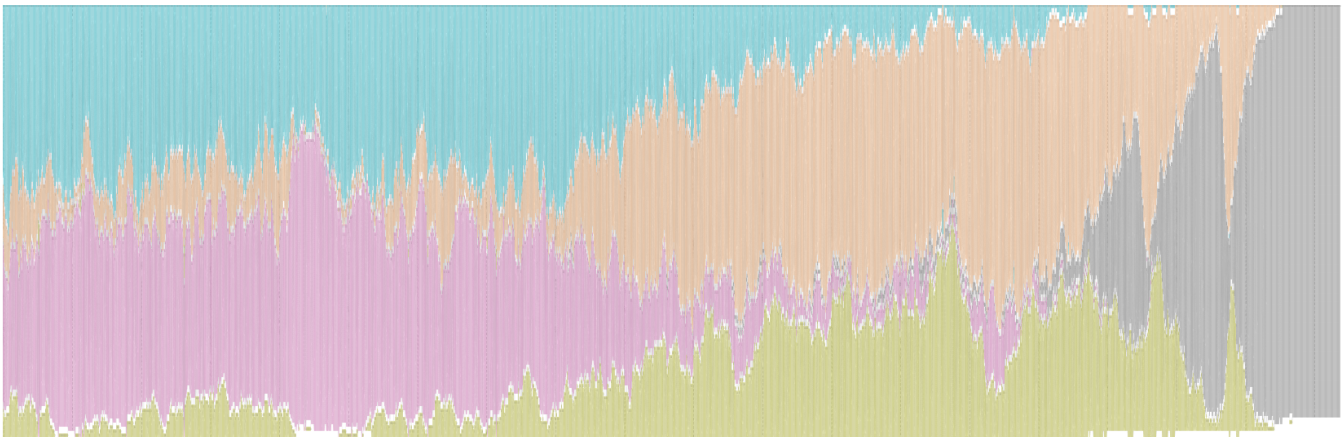

Figure 4: *Clustering Timeline covering the 100 members over all 1861 time steps (155 years) of the MPI-GE dataset.*

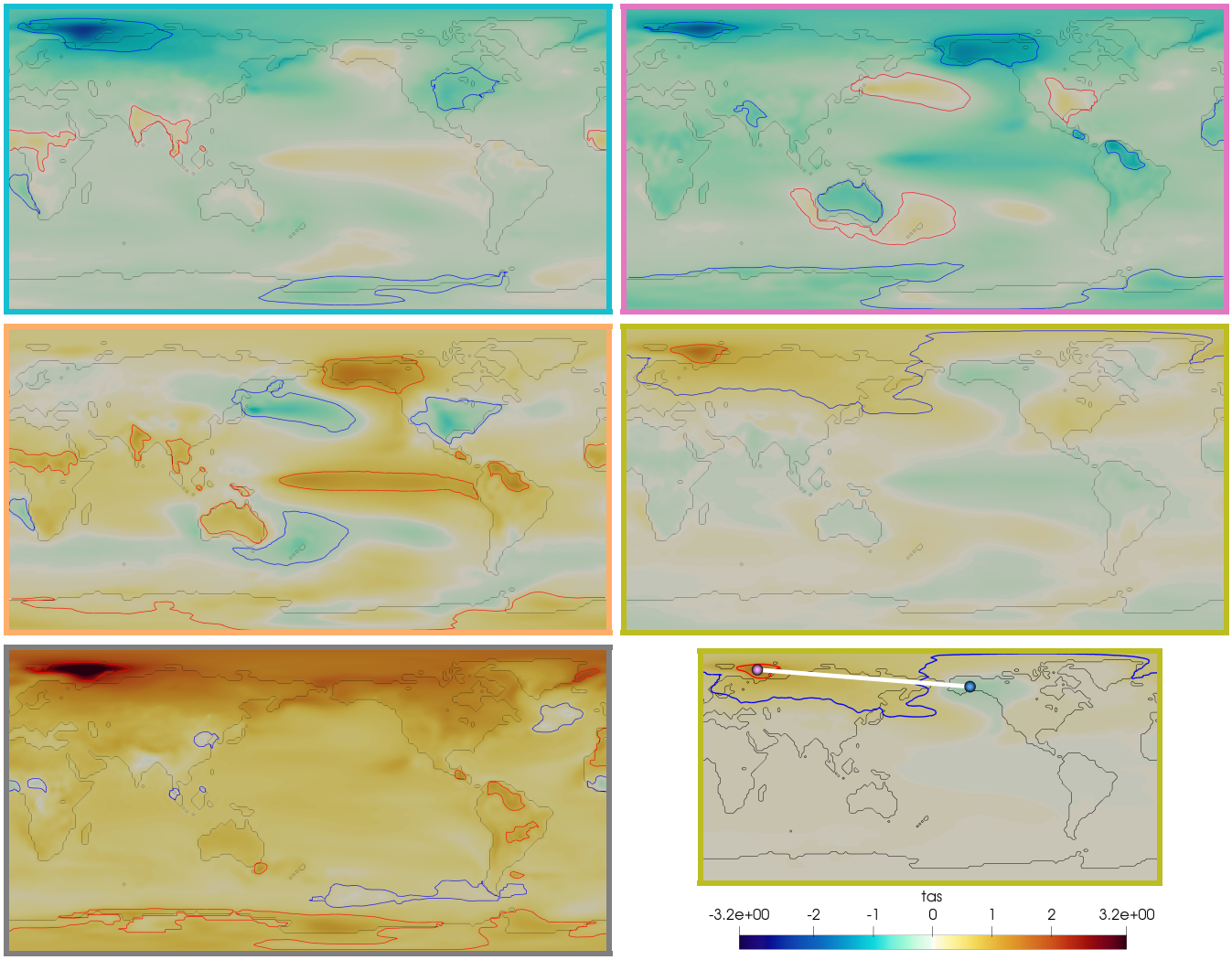

Figure 5: *The five time-independent clusters computed for the MPI-GE dataset. The respective frame color indicates which cluster from Figure 4 is shown. Bottom right: the green cluster after simplification.*

The green cluster (middle right) is so "neutral" (flat scalar field) that after the topological simplification only one minimum and one maximum is left, which in this case leads to one notable area of warming around the North Pole and one big negligible area of cooling that covers most of the rest of the planet.

In the image concerned with the last phase of the simulation (bottom left) we see a worldwide warming. Here, several small regions that are unusually cold are highlighted. Some of these may very well be important for the person interpreting this simulation result. Regarding their number and size, however, one might choose to filter some of them out by adjusting the size parameter.

5.2. Time-dependent

In a "frame-by-frame" analysis of time-dependent data, for the computation of cluster means only cluster members that stem from the current time step are considered (only a vertical slice of the Clustering Timeline).

Noteworthy about the analyzed ensemble is that during the first two phases it is divided into two rather contrasting clusters. In the mean taken over the complete ensemble, these opposing trends often cancel out. Our feature detection makes this particularly evident, as can be seen in Figure 6. The ensemble mean for the exemplary time step 359 (1880-05-31) exhibits only five features, three of which close to the north pole which is known to have quite extreme temperatures in these kinds of predictions. The feature detection for the two dominating clusters (bottom row) for this time step, however, highlights several regions that are likely to be of interest for a climate researcher. Among them are the El Niño and La Niña phenomenon (extraordinary warming/cooling in the Pacific Ocean, central in our maps), similarly contrasting predictions for the Sahel zone and – only in one cluster – cooling in northern Australia while its south coast is part of a region that is predicted to get warmer.

In the top right corner of Figure 6 we show a visualization of the ensemble mean field in the back, overlaid with the features found in the clusters. One can see the benefits of this approach: In a single picture the overall ensemble prediction is shown but the regions for which several members predict extreme conditions are highlighted by contours, the stroke color encoding whether there is a minimum or maximum of the scalar field. Partial-transparency of the contours of a cluster could indicate that its size is relatively small. But here all lines are completely opaque because the two considered clusters together make up almost the complete ensemble. We can see that in some parts (e.g. the northern hemisphere), the outlined features fit the ensemble mean quite well, although the field values are of course not as strong as in the respective cluster. Especially the opposite features, however, attract the user's attention. For example, the El Niño / La Niña prediction can be noted and further investigated.

We found the same utility for the second phase. The nodes of the domain-embedded contour tree in Figure 1 show that there are only two local minima and two local maxima in the simplified mean field. This is due to the roughly 50% influence of the rather neutral green cluster (see Figure 5 middle right). The orange cluster however contributes several interesting features to the central comparison view.

6. Discussion, conclusion and future work

We have found that the approach of deriving features in a scalar field based on the topology is well-suited for the analysis of climate data. Local extrema are a reliable characteristic for the patterns of climate phenomena whose appearance or absence in simulation ensembles are crucial for the evaluation of the data. The persistence and size filters can be used to capture just the right features for a dataset and the extent parameter works well for adjusting the feature regions to a reasonable size. Sometimes a good choice of parameters is tough, though. One threshold value for the simplification may not fit every field in a time-dependent ensemble. In order to detect features in a field with a generally low signal one may be tempted to lower the threshold but this is likely to lead to several false positives in fields with actually strong features. However, oversimplification (due to a high threshold) can lead to somewhat unintuitive results as in Figure 5 bottom right.

Several extensions based on this work could be developed in the future. The feature information could be exploited in a more comprehensive, interactive visualization setup; for example on clicking in the map, the system could tell the user if there are any extreme events predicted for this place, and if yes, which (how many) ensemble members contain this feature. To easily customize the feature detection to a specific dataset or specific research question, one could probably also use machine learning techniques to learn good values for the parameters with an expert user initially marking several feature regions manually. Concerning the MPI Grand Ensemble dataset, one could move on to analyze the subsets that cover the next 100 years and compare them with the historical data studied in this paper.

References

[BPR*15] Böttinger M., Pohlmann H., Röber N., Meier-Fleischer K., Spickermann D.: Visualization of 2d uncertainty in decadal climate predictions. In *Visualization in Environmental Sciences (EnvirVis), 2015. Workshop on* (2015), pp. 1–5. 2

[BRTM16] Bosler P. A., Roesler E. L., Taylor M. A., Mundt M. R.: Stride search: a general algorithm for storm detection in high-resolution climate data. *Geoscientific Model Development 9*, 4 (2016), 1383–1398. doi:10.5194/gmd-9-1383-2016. 2

[BSTS16] Bittner M., Schmidt H., Timmreck C., Sienz F.: Using a large ensemble of simulations to assess the northern hemisphere stratospheric dynamical response to tropical volcanic eruptions and its uncertainty. *Geophysical Research Letters 43*, 17 (Aug. 2016), 9324–9332. doi:10.1002/2016GL070587. 1, 2

[BTB15] Bauer P., Thorpe A., Brunet G.: The quiet revolution of numerical weather prediction. *Nature 525* (Sep 2015), 47 EP –. Review Article. URL: https://doi.org/10.1038/nature14956. 1

[CSvdP10] Carr H., Snoeyink J., van de Panne M.: Flexible isosurfaces: Simplifying and displaying scalar topology using the contour tree. *Computational Geometry 43*, 1 (2010), 42–58. Special Issue on the 14th Annual Fall Workshop. URL: http://www.sciencedirect.com/science/article/pii/S0925772109000455, doi:10.1016/j.comgeo.2006.05.009. 3

[ELZ00] Edelsbrunner H., Letscher D., Zomorodian A.: Topological persistence and simplification. In *Proceedings 41st Annual Symposium on Foundations of Computer Science* (Nov. 2000), IEEE, pp. 454–463. doi:10.1109/SFCS.2000.892133. 3

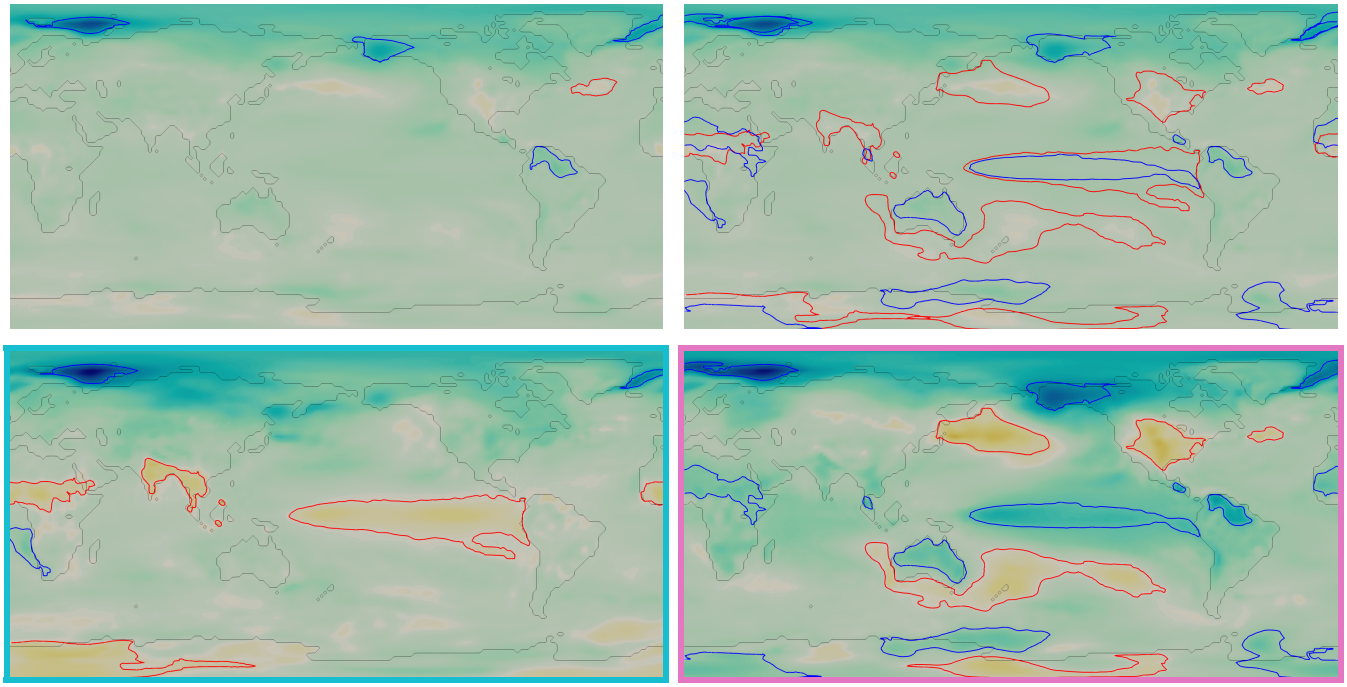

Figure 6: *Time 1880-05-31 in the MPI-GE dataset. Top left: ensemble mean; bottom: the two main clusters (blue and pink in Figure 4); top right: ensemble mean with contours for the two main clusters.*

[FFST19] FAVELIER G., FARAJ N., SUMMA B., TIERNY J.: Persistence atlas for critical point variability in ensembles. *IEEE Transactions on Visualization and Computer Graphics 25*, 1 (Jan. 2019), 1152–1162. doi:10.1109/TVCG.2018.2864432. 3

[GFJT17] GUEUNET C., FORTIN P., JOMIER J., TIERNY J.: Task-based augmented merge trees with fibonacci heaps. In *2017 IEEE 7th Symposium on Large Data Analysis and Visualization (LDAV)* (Oct. 2017), IEEE, pp. 6–15. doi:10.1109/LDAV.2017.8231846. 2

[GMH92] GONG P., MARCEAU D. J., HOWARTH P. J.: A comparison of spatial feature extraction algorithms for land-use classification with SPOT HRV data. *Remote Sensing of Environment 40*, 2 (1992), 137–151. 2

[Has93] HASSELMANN K.: Optimal fingerprints for the detection of time-dependent climate change. *Journal of Climate 6*, 10 (1993), 1957–1971. doi:10.1175/1520-0442(1993)006<1957:OFFTDO>2.0.CO;2. 3

[HFBG17] HÜTTENBERGER L., FEIGE K., BÖTTINGER M., GARTH C.: Analyzing climate simulation ensembles using pareto sets. In *IEEE Vis2017* (2017). 3

[HJS07] HANNACHI A., JOLLIFFE I. T., STEPHENSON D. B.: Empirical orthogonal functions and related techniques in atmospheric science: A review. *International Journal of Climatology 27*, 9 (2007), 1119–1152. URL: http://dx.doi.org/10.1002/joc.1499, doi:10.1002/joc.1499. 3

[HLH*16] HEINE C., LEITTE H., HLAWITSCHKA M. W., IURICICH F., DE FLORIANI L., SCHEUERMANN G., HAGEN H., GARTH C.: A survey of topology-based methods in visualization. *Computer Graphics Forum 35*, 3 (2016), 643–667. URL: http://dx.doi.org/10.1111/cgf.12933, doi:10.1111/cgf.12933. 2

[Hod94] HODGES K. I.: A general method for tracking analysis and its application to meteorological data. *Monthly Weather Review 122*, 11 (1994), 2573–2586. doi:10.1175/1520-0493(1994)122<2573:AGMFTA>2.0.CO;2. 2

[HvSH*96] HEGERL G. C., VON STORCH H., HASSELMANN K., SANTER B. D., CUBASCH U., JONES P. D.: Detecting greenhouse-gas-induced climate change with an optimal fingerprint method. *Journal of Climate 9*, 10 (1996), 2281–2306. doi:10.1175/1520-0442(1996)009<2281:DGGICC>2.0.CO;2. 3

[KBL18] KAPPE C. P., BÖTTINGER M., LEITTE H.: Exploring variability within ensembles of decadal climate predictions. *IEEE Transactions on Visualization and Computer Graphics* (2018). URL: doi.ieeecomputersociety.org/10.1109/TVCG.2018.2810919, doi:10.1109/TVCG.2018.2810919. 3, 4

[Llo82] LLOYD S.: Least squares quantization in pcm. *IEEE Transactions on Information Theory 28*, 2 (1982), 129–137. 4

[LW07] LU D., WENG Q.: A survey of image classification methods and techniques for improving classification performance. *International Journal of Remote Sensing 28*, 5 (2007), 823–870. doi:10.1080/01431160600746456. 2

[MHS*96] MANDERS E. M. M., HOEBE R. A., STRACKEE J., VOSSEPOEL A. M., ATEN J. A.: Largest contour segmentation: A tool for the localization of spots in confocal images. *Cytometry 23*, 1 (1996), 15–21. doi:10.1002/(SICI)1097-0320(19960101)23:1<15::AID-CYTO3>3.0.CO;2-L. 3, 4

[MMS*94] MESROBIAN E., MUNTZ R. R., SANTOS J. R., SHEK E. C., MECHOSO C. R., FARRARA J. D., STOLORZ P.: Extracting spatio-temporal patterns from geoscience datasets. In *Proceedings of Workshop on Visualization and Machine Vision* (June 1994), IEEE, pp. 92–103. doi:10.1109/VMV.1994.324983. 2

[OBJ16] OBERMAIER H., BENSEMA K., JOY K. I.: Visual trends analysis in time-varying ensembles. *IEEE Transactions on Visualization and Computer Graphics 22*, 10 (2016), 2331–2342. 3

[RBS*18] RAUTENHAUS M., BÖTTINGER M., SIEMEN S., HOFFMAN R., KIRBY R. M., MIRZARGAR M., RÖBER N., WESTERMANN R.: Visualization in meteorology—a survey of techniques and tools for

data analysis tasks. *IEEE Transactions on Visualization and Computer Graphics 24*, 12 (Dec 2018), 3268–3296. doi:10.1109/TVCG.2017.2779501. 2

[SHCS13] SCHNEIDER D., HEINE C., CARR H., SCHEUERMANN G.: Interactive comparison of multifield scalar data based on largest contours. *Computer Aided Geometric Design 30*, 6 (2013), 521–528. Foundations of Topological Analysis. URL: http://www.sciencedirect.com/science/article/pii/S0167839612000490, doi:https://doi.org/10.1016/j.cagd.2012.03.023. 3

[Sil95] SILVER D.: Object-oriented visualization. *IEEE Computer Graphics and Applications 15*, 3 (May 1995), 54–62. doi:10.1109/38.376613. 3

[Ste15] STEVENS B.: Rethinking the lower bound on aerosol radiative forcing. *Journal of Climate 28*, 12 (June 2015), 4794–4819. MPI-GE. doi:10.1175/JCLI-D-14-00656.1. 2

[SWC*08] SCHNEIDER D., WIEBEL A., CARR H., HLAWITSCHKA M., SCHEUERMANN G.: Interactive comparison of scalar fields based on largest contours with applications to flow visualization. *IEEE Transactions on Visualization and Computer Graphics 14*, 6 (2008), 1475–1482. 3

[TFL*18] TIERNY J., FAVELIER G., LEVINE J. A., GUEUNET C., MICHAUX M.: The Topology ToolKit. *IEEE Transactions on Visualization and Computer Graphics 24*, 1 (Jan. 2018), 832–842. https://topology-tool-kit.github.io/. doi:10.1109/TVCG.2017.2743938. 4

[TP12] TIERNY J., PASCUCCI V.: Generalized topological simplification of scalar fields on surfaces. *IEEE Transactions on Visualization and Computer Graphics 18*, 12 (Dec. 2012), 2005–2013. doi:10.1109/TVCG.2012.228. 3

[Wil81] WILLIAMSON D. L.: Storm track representation and verification. *Tellus 33*, 6 (1981), 513–530. doi:10.1111/j.2153-3490.1981.tb01778.x. 2